Enhanced vascular permeability facilitates entry of plasma HDL and promotes macrophage-reverse cholesterol transport from skin in mice

Ilona Kareinen,* Lídia Cedó,† Reija Silvennoinen,* Pirkka-Pekka Laurila,§ Matti Jauhiainen,§ Josep Julve,† Francisco Blanco-Vaca,† Joan Carles Escola-Gil,† Petri T. Kovanen,[1,*] and Miriam Lee-Rueckert*

Wihuri Research Institute,* Helsinki, Finland; IIB Sant Pau, Departament de Bioquímica i Biologia Molecular,† Universitat Autònoma de Barcelona-CIBER de Diabetes y Enfermedades Metabolicas Asociadas, Barcelona, Spain; and Public Health Genomics Unit,§ National Institute for Health and Welfare, Helsinki, Finland

Abstract Reverse cholesterol transport (RCT) pathway from macrophage foam cells initiates when HDL particles cross the endothelium, enter the interstitial fluid, and induce cholesterol efflux from these cells. We injected [^{3}H] cholesterol-loaded J774 macrophages into the dorsal skin of mice and measured the transfer of macrophage-derived [^{3}H]cholesterol to feces [macrophage-RCT (m-RCT)]. Injection of histamine to the macrophage injection site increased locally vascular permeability, enhanced influx of intravenously administered HDL, and stimulated m-RCT from the histamine-treated site. The stimulatory effect of histamine on m-RCT was abolished by prior administration of histamine H1 receptor (H1R) antagonist pyrilamine, indicating that the histamine effect was H1R-dependent. Subcutaneous administration of two other vasoactive mediators, serotonin or bradykinin, and activation of skin mast cells to secrete histamine and other vasoactive compounds also stimulated m-RCT. None of the studied vasoactive mediators affected serum HDL levels or the cholesterol-releasing ability of J774 macrophages in culture, indicating that acceleration of m-RCT was solely due to increased availability of cholesterol acceptors in skin. We conclude that disruption of the endothelial barrier by vasoactive compounds enhances the passage of HDL into interstitial fluid and increases the rate of RCT from peripheral macrophage foam cells, which reveals a novel tissue cholesterol-regulating function of these compounds.—Kareinen, I., L. Cedó, R. Silvennoinen, P-P. Laurila, M. Jauhiainen, J. Julve, F. Blanco-Vaca, J. C. Escola-Gil, P. T. Kovanen, and M. Lee-Rueckert. **Enhanced vascular permeability facilitates entry of plasma HDL and promotes macrophage-reverse cholesterol transport from skin in mice. *J. Lipid Res.* 2015.** 56: **241–253.**

Supplementary key words bradykinin • cholesterol • foam cells • high density lipoprotein • histamine • lipoproteins • mast cells • serotonin

Vascular endothelium is a semipermeable barrier that regulates the solute composition of interstitial fluids by an ultrafiltration process of various blood components (1). Such a sieving effect also determines the passage through the endothelium of the various types of lipoproteins, which are the largest blood solutes. It was an early observation in hypercholesterolemic rabbits that the arterial influx of plasma HDL, LDL, and VLDL decreases linearly with the logarithm of the diameter of the lipoprotein particles (2). Studies in humans and other mammalian species also indicated that the flux of LDL from plasma into the arterial wall depends not only on its plasma concentration but also on its permeability at the plasma-arterial wall interface (3).

Accumulation of excess cholesterol in cytoplasmic lipid droplets of macrophages in the arterial intima is a primary event in atherosclerosis. Accordingly, an efficient control of the cholesterol pool in the arterial foam cells is essential to prevent progression of the disease or even to induce its regression. In general, control of cellular cholesterol balance is partially achieved by the transfer of cellular cholesterol from peripheral body compartments to the liver and ultimately to the gut for its fecal excretion along a pathway that is known as the reverse cholesterol transport (RCT) (4). Efflux of cellular

The Wihuri Research Institute is maintained by the Jenny and Antti Wihuri Foundation. This work was supported by the Finnish Foundation of Veterinary Research (I.K.) and partly funded by the Ministerio de Sanidad y Consumo, Instituto de Salud Carlos III, FIS 12-00291. CIBER de Diabetes y Enfermedades Metabólicas Asociadas is an Instituto de Salud Carlos III Project.

Manuscript received 11 November 2014 and in revised form 2 December 2014.

Published, JLR Papers in Press, December 3, 2014
DOI 10.1194/jlr.M050948

Abbreviations: apoA-I-KO, apoA-I-deficient; H1R, histamine H1 receptor; H2R, histamine H2 receptor; LDLr-KO, LDL receptor-deficient; LSC, liquid scintillation counting; m-RCT, macrophage-RCT; RCT, reverse cholesterol transport; SR-BI, scavenger receptor class B type I; 48/80, compound 48/80.

[1] To whom correspondence should be addressed.
e-mail: petri.kovanen@wri.fi

cholesterol to HDL initiates RCT in all tissues, but only the tiny fraction of the total body RCT that originates in the cholesterol-loaded macrophage foam cells [macrophage-RCT (m-RCT)] located in the intima is directly involved in atherosclerosis (5). It currently appears that the dynamics of the cholesterol flux induced from macrophage foam cells to feces by HDL particles, and their main apolipoprotein constituent apoA-I, is critical for their cardioprotective function (6). Indeed, the capability of HDL to induce regression of atherosclerosis has been demonstrated in clinical studies in which infusion of apoA-I-containing reconstituted HDL reduced the atheroma volume or improved the plaque characterization score in patients who had suffered an acute coronary syndrome (7, 8).

The skin is the largest organ of the body, and its cholesterol content has been directly associated with an increased carotid intima-media thickness in individuals without diagnosed cardiovascular disease, suggesting that measuring skin cholesterol content may be useful when attempting to identify individuals with subclinical asymptomatic atherosclerosis (9–11). Importantly, because deposition of cholesterol in skin xanthomas and in early atherosclerotic lesions has been suggested to share common pathogenic mechanisms (12), a close resemblance can be postulated between skin and the intimal layer of human arteries, two sites where foam cells are formed. In cells that reside in peripheral tissues such as the skin, RCT is initiated by the cholesterol efflux-inducing abilities of the HDL particles present in the cutaneous interstitial fluid. Notably, it has been recently found that the lymphatic vasculature, by facilitating removal of HDL from interstitial fluids, stimulates cholesterol clearance from the skin and the arterial wall and, accordingly, enables RCT from these sites (13, 14). These observations support the notion that an impaired outward flow of HDL from the interstitial fluid to lymph shares common features in the skin and the arterial wall and so influences cholesterol balance in these two tissues.

We have previously shown that an increase in the endothelial permeability of dorsal skin sites in rats induced by histamine increases the transendothelial passage of plasma LDL to the affected sites (15). Here, we hypothesize that an increase in the transendothelial passage of circulating HDL into tissue sites in which foam cells are present would enhance the local interstitial pool of HDL and promote m-RCT. To test this hypothesis, we evaluated the effect of increased vascular permeability in the skin on the rate of RCT from J774 foam cells injected into the dorsal subcutaneous layer of the skin in mice. We found that increasing the subcutaneous levels of inflammatory mediators capable of increasing endothelial permeability, namely histamine, serotonin, and bradykinin, locally stimulated uptake of HDL by the skin and also accelerated the rate of m-RCT from skin to feces. The present results reveal that sole stimulation of HDL transfer from plasma to peripheral interstitial fluids is capable of promoting m-RCT in vivo.

MATERIALS AND METHODS

Materials

Evans blue dye, histamine, serotonin, bradykinin, the mast cell-degranulating compound 48/80 (48/80), the histamine H1 receptor (H1R) antagonist pyrilamine, and the histamine H2 receptor (H2R) antagonist ranitidine were purchased from Sigma Aldrich. [1α,2α(n)-^{3}H]cholesterol (specific activity 40–60/mmol) was purchased from Perkin Elmer.

Animals

C57BL/6JOlaHsd mice (age 9–12 weeks) were purchased from Harlan Laboratories (Venray, Holland). ApoA-I-deficient (apoA-I-KO) mice on the C57BL/6J background (age 20–30 weeks) were kindly provided by Dr. Jesús Osada (University of Zaragoza, Spain) and LDL receptor-deficient (LDLr-KO) mice (age 9–16 weeks) on the C57BL/6J background were obtained from Jackson Laboratory (Bar Harbor, ME; Stock Number: 002207). Mice were housed in groups of five per cage, allowed to access regular chow rodent diet (Teklad Global, Harlan Laboratories) and water ad libitum and were maintained in an automatic 12/12 h dark-light cycle. All experiments were conducted in compliance with national guidelines for the care and use of research animals, and the experimental protocols were approved by the Animal Experiment Board of Finland (ELLA) and by the Institutional Animal Care Committee of the Institut de Recerca de l'Hospital de la Santa Creu I Sant Pau, Spain.

Skin permeability test and measurement of the histamine content of skin

The fur on the dorsal back was shaved 2 days prior the experiment to prevent skin irritation on the experimental day. For the permeability test, mice were given an intraperitoneal injection of Evans blue dye in saline (2%; 4 ml/kg) (16), and the dye was allowed to circulate for 4 h. After 30 min of Evans blue administration, mice received subcutaneous injection of histamine (250 μg/kg in 100 μl saline) or vehicle alone in the rostral back. The degree of Evans blue extravasation was quantitated by measuring the formed blue-colored circle at 0.5, 1, 2, 3, and 4 h and documenting it by photography. The skin content of histamine was measured after 1 h of subcutaneous injection of histamine or vehicle. Mice were euthanized, and a piece of skin (area of 1 cm^2) was dissected from the injection site, weighted, and chopped up with scissors. The finely cut pieces were placed in 500 μl of distilled water in Eppendorf tubes and then subjected to five freeze-thaw cycles (liquid nitrogen-warm tap water). TCA was then added to the tubes (final concentration 5%), after which they were thoroughly vortexed, incubated at +4°C for 30 min, and finally centrifuged at 10,000 *g* for 10 min. The clear supernatant was collected, the histamine content was determined fluorometrically (17), and the results were expressed as nanograms of histamine per area and per weight of skin.

Measurement of mast cell activation in skin

To induce degranulation of mast cells in the skin, 48/80 (2.5 mg/kg) was subcutaneously injected to mice. Mast cells were defined to be activated when extracellular granules were found in the immediate vicinity of the cells. For quantification of the number of activated mast cells, a piece of skin was cut from the treated skin sites and submerged in the tissue section medium Tissue-Tek OCT (Sakura Finetek Europe). The skin samples were then rapidly frozen in liquid nitrogen and stored at −80°C to be further sectioned into 5 μm slices. The slices were stained in 0.1% Toluidine Blue, and the number of activated mast cells was

determined microscopically at 20× and expressed as percent of the total number of mast cells, as described previously (18).

Stimulation of the vascular permeability of mice

The targeted site of skin for the multiple subcutaneous injections was confined to a skin area of a diameter of about 1 cm in the rostral back between the scapulae. Mice received subcutaneous injections of either histamine (250 μg/kg), serotonin (500 μg/kg), or bradykinin (500 μg/kg) in 100 μl of saline, or vehicle alone as control. To further stimulate vascular permeability, the same dose of each respective compound was administered after 24 h of the initial dose. To block the H1R or the H2R, or both, mice were intraperitoneally injected with either pyrilamine (20 mg/kg), ranitidine (20 mg/kg), or with both histamine receptor antagonists, respectively, 1 h prior to histamine injection. Each experiment with the vasoactive compounds was repeated at least two times, and the number of mice ranged from 10 to 15 per treatment, as indicated in the figure legends.

[^{3}H]HDL serum kinetics and uptake by skin and other tissues

HDL (d = 1.063–1.21 g/ml) were isolated by ultracentrifugation from pooled sera derived from control mice and were tritium-labeled in their protein component by the Bolton-Hunter procedure to yield [^{3}H]HDL (19). Mice received subcutaneous injections of histamine, serotonin, bradykinin, or vehicle, as described above, and then immediately an intravenous injection of the [^{3}H]HDL preparation (2.2–5.1 × 10^4 dpm/μg HDL protein) via the tail vein (∼50 μg HDL protein/mouse, 1.2–2.8 × 10^6 dpm/mouse). Minimal volume of blood (ranging from 10 to 50 μl) was drawn from the saphenous vein at 2 min, 30 min, 60 min, 3 h, 24 h, and 48 h. Plasma decay curves for the tracer were normalized to the serum radioactivity determined at the 2 min time point after injection of the radioactive tracer. Mice were euthanized at 1 h, 24 h, and 48 h, and samples of skin were dissected from the site of the subcutaneous injection. Tissues were rinsed with saline, finely chopped, and incubated overnight in 1 ml of 2 N KOH at 37°C. Radioactivity in serum and tissue extracts was measured by liquid scintillation counting (LSC).

Evaluation of m-RCT from skin to feces

We determined the in vivo m-RCT rate from skin to feces within a 48 h period, as previously described (20). In brief, [^{3}H] cholesterol-labeled J774 mouse macrophages (3–5 × 10^6 cells; 2–5 × 10^6 dpm per mouse) were subcutaneous injected into the rostral back area of mice, and immediately thereafter, the various vasoactive compounds were injected into an adjacent skin site. To further stimulate vascular permeability, the dose of each vasoactive compound was administered two times within a 48 h period, as described above. After the treatments, mice were maintained for 48 h in individual mesh bottom cages to quantitatively collect the fecal material. Finally, mice were exsanguinated by cardiac puncture under terminal isoflurane anesthesia and livers removed after rinsing with saline. Total serum [^{3}H]cholesterol radioactivity and HDL-associated [^{3}H] cholesterol radioactivity were determined by LSC after precipitation of apoB-lipoproteins with phosphotungstic acid and magnesium chloride (Roche Diagnostics GmbH, Germany), as previously described (20). Total hepatic and fecal lipids were extracted with isopropanol:hexane. The lipid-containing layer was collected, solvent was evaporated, and [^{3}H]tracer radioactivity was measured by LSC. The [^{3}H]tracer detected in fecal bile acids was determined in the remaining aqueous portion of the fecal extracts. The quantity of [^{3}H]tracer in each compartment was expressed as a fraction of the injected dose. In other experiments, the m-RCT rate from skin to feces was evaluated in wild-type mice upon triggering release of endogenous histamine in skin by subcutaneous dose of 48/80 (2.5 mg/kg) and in histamine-treated LDLr-KO mice. We also evaluated the effect of histamine in the setting of low HDL levels. In this experiment, apoA-I-KO mice were treated with the studied subcutaneous dose of histamine followed by an intravenous injection of HDL (100–150 μg protein, 95–145 nmol cholesterol) isolated from wild-type mice, which partly (∼20%) and transiently reconstituted the basal levels of HDL-cholesterol in these mice, which were 0.6–0.8 mM. Groups of mice that received only subcutaneous histamine or only intravenous HDL acted as reference groups.

Gene expression of cholesterol efflux transporters in cultured J774 macrophages and determination of macrophage cholesterol efflux to mouse serum in vitro

J774 cells were cultured in RPMI 1640 medium supplemented with 10% FBS, 100 U/ml penicillin, and 100 U/ml streptomycin (BioWhittaker, Verviers, Belgium), seeded in 12-well plates at 5 × 10^5 cells/well, and grown for 3 days. To mimic the in vivo flow and ensuing dilution and predicted decline in concentration of the subcutaneous injected compounds (histamine, serotonin, bradykinin) occurring in the interstitial fluid of the skin to which the labeled macrophages were exposed, the J774 cells were incubated with decreasing concentrations of each compound for various intervals of time, up to 3 h. Accordingly, the initial concentration of each compound in the incubation medium was the same as that injected to the mice; after 5 min of incubation, the compound concentration was progressively reduced within intervals of 10 min to achieve up to a 100-fold reduction at 30 min of incubation. After such a 30 min preconditioning period, the incubation was prolonged until 3 h at this low concentration. Macrophages incubated in only medium (nonconditioned cells) acted as controls. The preconditioned cells were then collected for quantitative RT-PCR analysis. Total RNA was isolated using RNeasy Plus Mini Kit (Qiagen, Hilden, Germany). cDNA was generated using Oligo(dT)23 (Sigma-Aldrich, St. Louis, MO) and M-MLV Reverse Transcriptase, RNase H Minus, Point Mutant (Promega, Madison, WI) and was subjected to quantitative RT-PCR amplification using the TaqMan Master Mix (Applied Biosystems, Foster City, CA). Specific TaqMan probes (Applied Biosystems) were used for each gene: Mm00442646_m1 for *Abca1*, Mm00437390_m1 for *Abcg1*, and Mm00450236_m1 for *Scarb1* [scavenger receptor class B type I (SR-BI)]. *Gapdh* was used as the reference gene (Mm99999915_g1). Reactions were run on a CFX96™ Real-Time System (Bio-Rad, Hercules, CA) according to the manufacturer's instructions. The relative mRNA expression levels were calculated using the ΔΔCt method.

In a parallel experiment, in vitro cholesterol efflux from [^{3}H] cholesterol-labeled J774 macrophage foam cells was determined after the cells had been preconditioned for 30 min with decreasing concentrations of the vasoactive compounds, as described above. For this purpose, aliquots of the normal pool of mouse serum (2.5% final concentration in medium) were added to the preconditioned macrophages in media containing the respective vasoactive compound at the final (100-fold reduced) concentration, and cholesterol efflux was determined during a 3 h incubation period. Efflux from nonconditioned macrophages to mouse serum in the absence of vasoactive compounds acted as the reference. Fractional cholesterol efflux (%) was calculated as dpm_{medium} /(dpm_{cells} + dpm_{medium}) × 100, as described before (20). Efflux values in the absence of serum were subtracted from those in the presence of serum.

Other analyses

Total cholesterol, HDL-cholesterol, and triglyceride concentrations in mouse serum were measured enzymatically with commercial kits (Roche Diagnostics, Basel, Switzerland).

Statistical analysis

GraphPad Prism 4.0 software (GraphPad, San Diego, CA) was used to perform all statistical analyses. Unpaired *t*-test with Welch's correction was used to evaluate statistical differences between two groups. One-way ANOVA with Bonferroni's multiple comparison test was used to compare data from three or more groups. A P value <0.05 was considered statistically significant. All data are expressed as the mean ± SEM.

RESULTS

Subcutaneous injection of histamine rapidly increases the transport of Evans blue from blood to skin

We first evaluated the time dependency of subcutaneous dose of histamine (250 μg/kg), a well-known vasodilator agent, to induce vascular permeability in the skin of mice. For this purpose, mice received an intraperitoneal injection of Evans blue dye and 30 min later subcutaneous injections of histamine or saline into the interscapular area of the back. Histamine induced a fast (within 10 min) local permeability reaction reflected by the appearance of a blue-colored area in the skin around the injection site, whereas injection of saline alone was without effect (n = 5 mice/group). The diameters of the colored circles in the histamine-treated mice were 16 ± 2.4 mm (at 10 min) and 18 ± 3.3 mm (at 30 min). One hour after histamine injection, it was no more possible to measure accurately the magnitude of the generated area because of extensive diffusion of the dye in the dorsal skin. Moreover, at that time the histamine contents in the treated skin areas were equally low in histamine-treated and vehicle-treated mice (0.39 ± 0.02 and 0.38 ± 0.04 ng/mg of skin, respectively; n = 6 mice/group), reflecting fast removal of the injected histamine from the injection site.

Histamine markedly stimulates fecal excretion of [^{3}H] cholesterol from subcutaneously injected macrophage foam cells

To test whether the histamine-mediated increase of vascular permeability in the skin was capable of modifying the RCT rate from macrophages located in the subcutaneous layer of the skin, [^{3}H]cholesterol-labeled macrophages were subcutaneously injected, and immediately thereafter, histamine was injected into the same tissue site. In preliminary experiments, we observed that a single dose of histamine induced only a nonsignificant increase in the overall m-RCT rate to feces relative to the vehicle group (0.72 ± 0.23 vs. 0.48 ± 0.06% of the injected dose, P = 0.32, n = 8 mice/group) within the 48 h period. This failure could be related to the rapid and only transient local effect of histamine in the skin. Thus, in the following experiments, mice received a second subcutaneous dose of histamine at 24 h after the first dose, all various injection sites being closely located within the target skin area. After 48 h of injection of the cells, the transfer of macrophage-derived [^{3}H]cholesterol to feces was evaluated (**Fig. 1**). In comparison with control mice that received only vehicle, treatment with histamine significantly increased the content of radiolabeled cholesterol in serum and HDL and also tended to increase it in the liver (Fig. 1A, B). More importantly, the quantity of macrophage-derived [^{3}H]cholesterol excreted into feces during the 48 h period was 2-fold higher in these mice in which the immediate vasoactive histamine stimulus was repeated at 24 h (Fig. 1C). We further evaluated whether the effect of histamine on m-RCT involved the H1R and/or H2R, which have been shown to stimulate the transendothelial transport of LDL from plasma to skin of rats in vivo (15). For this purpose, mice received 1 h before the histamine dose an intraperitoneal injection of either pyrilamine or ranitidine to antagonize H1R and H2R, respectively, and the fecal recovery of the macrophage-derived ^{3}H-radioactivity was measured. As shown in **Fig. 2**, the stimulatory effect of histamine on the m-RCT from skin to feces was significantly reduced when the H1R antagonist

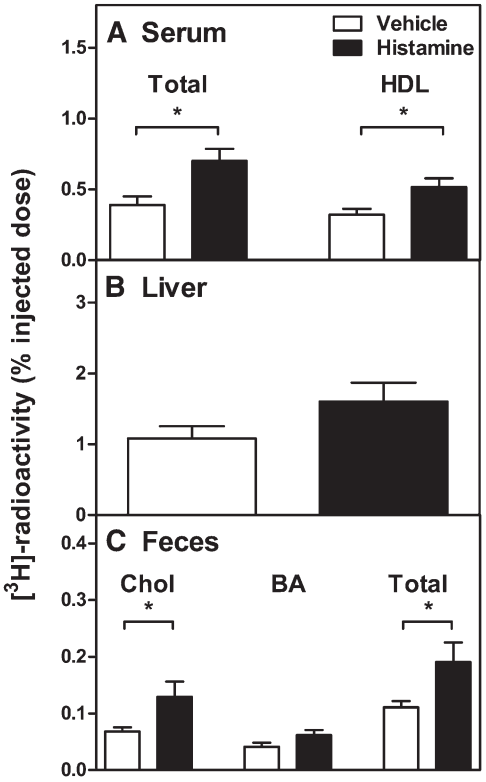

Fig. 1. Histamine stimulates in vivo m-RCT from skin to feces. Mice received subcutaneous injection of [^{3}H]cholesterol-labeled J774 foam cells immediately followed by subcutaneous injection of histamine (250 μg/kg) or vehicle. The same subcutaneous dose of histamine or vehicle was repeated after 24 h of the initial injection. The transfer of macrophage-derived [^{3}H]cholesterol from the skin to serum (A), liver (B), and feces (C) was determined by measuring the radioactivity in each compartment after 48 h. Excretion of the total tracer in feces corresponds to the [^{3}H]cholesterol and [^{3}H]bile acid fractions. Data represent the mean ± SEM from three independent experiments. Statistical significance relative to the vehicle group is denoted as * P < 0.05; n = 15 mice/group.

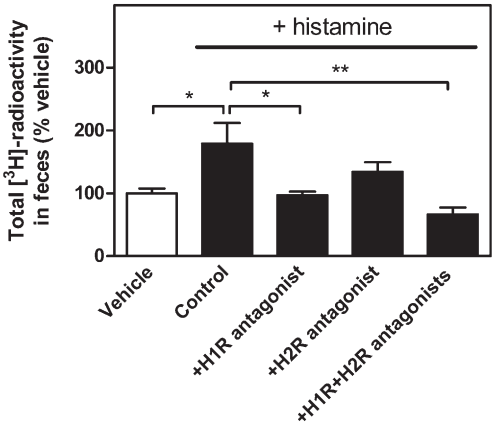

Fig. 2. H1R is involved in the histamine-dependent effect on m-RCT. Mice received subcutaneous injection of [^{3}H]cholesterol-labeled J774 macrophage foam cells immediately followed by subcutaneous injection of histamine (250 μg/kg) or vehicle. To block H1R or H2R, or both, mice were injected intraperitoneally with either pyrilamine (20 mg/kg), ranitidine (20 mg/kg), or both histamine receptor antagonists 1 h prior to the histamine dose. Mice that received vehicle alone acted as a reference to evaluate the basal m-RCT. Treatments with histamine alone (control) and with both histamine and its antagonists were repeated 24 h after the initial doses. The rate of m-RCT from skin to feces was determined after 48 h of injection of the cholesterol-labeled cells by measuring the excretion of [^{3}H]radioactivity in feces ([^{3}H]cholesterol + [^{3}H]bile acids). Data represent the mean ± SEM from two independent experiments and were normalized as percent of control (vehicle). Mean value obtained in the vehicle group was 0.13 ± 0.01, and it was set as 100%. Statistical significance is denoted as * $P < 0.05$, ** $P < 0.01$; n = 10 mice/group for vehicle and control, and n = 4–5 mice/group for the histamine antagonist groups.

was administered, and only slightly reduced when the H2R antagonist was administered. When administered together, the two antagonists exhibited a stronger effect, which supported the notion that the H2 antagonist had a small additive effect when combined with the H1 antagonist. Yet, no statistical difference was found between the values obtained when blocking only H1R or blocking both H1R and HR2. Overall these results indicated that the histamine-dependent effect on m-RCT was mainly mediated by H1R.

Histamine increases influx of HDL to skin

To get insight into the mechanism by which histamine induced m-RCT from the treated skin, we evaluated the capability of the locally injected histamine to induce the influx of [^{3}H]HDL from plasma into the skin within 48 h (i.e., the time period in which m-RCT rate was measured). Because the tissue content of HDL is determined at any moment by the magnitudes of the simultaneously occurring inflow into and the outflow from the extracellular fluid in the treated tissue site, it is not possible to determine the exact magnitude of the vascular leakage in the treated skin site at various time points. Thus, we measured the total content of radioactivity in the studied skin site, which is an approximation of the concentration of the labeled HDL in the extracellular fluid of the tissue site and also the determinant of the local cellular cholesterol efflux-inducing capacity of HDL in vivo. For this purpose, we isolated mouse HDL, radiolabeled the protein component of the isolated HDL, and intravenously injected the [^{3}H]HDL into mice immediately after the animals had received subcutaneous injection of histamine or vehicle. After 1 h, 24 h, and 48 h, the mice were euthanized, the treated sites of skin were collected, and their contents of ^{3}H-radioactivity were measured. As shown in **Fig. 3A**, the local effect on skin permeability induced by subcutaneous injection of histamine did not modify the clearance kinetics of the circulating pool of [^{3}H]HDL. Importantly, a significant 3-fold increase in the flux of [^{3}H]HDL into the histamine injection skin site was observed within 1 h (Fig. 3B). Because, to promote m-RCT, the HDL particles that entered the skin site must leave the site, we measured the levels of [^{3}H]HDL in skin at prolonged time points, at 24 h and 48 h. Notably, the [^{3}H]HDL content in the skin of the histamine-treated mice decreased to the level of the control mice within 24 h of histamine injection indicating that during this period HDL had left the skin site, and no further changes were observed at 48 h. Overall, the results

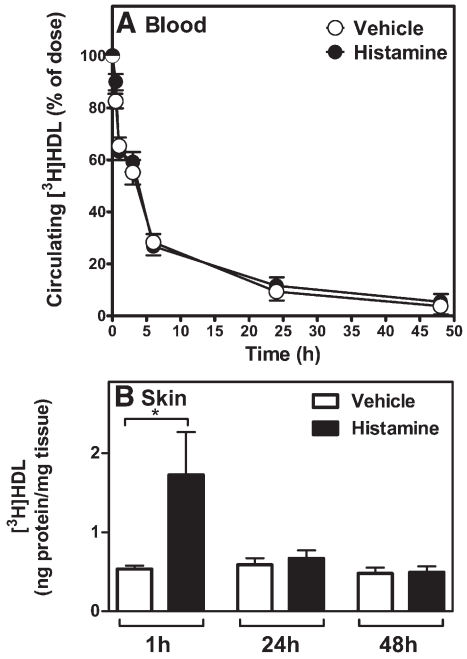

Fig. 3. Histamine facilitates the influx of [^{3}H]HDL to skin. HDL was isolated from pooled serum from control mice, and [^{3}H]HDL was prepared by labeling the protein component. Mice received subcutaneous injections of histamine or vehicle, as described in Fig. 1, immediately followed by intravenous injection of the labeled HDL preparation via the tail vein. Blood was drawn from the saphenous vein at 2 min, 30 min, 1 h, 3 h, 6 h, 24 h, and 48 h. Decay curves for the tracer in blood were expressed as percent of the radioactivity at the 2 min time point after injection of the tracer (A). Samples of skin were dissected from the site of subcutaneous injection at 1 h, 24 h, and 48 h after the intravenous administration of [^{3}H]HDL. Radioactivity was measured in tissue extracts, and the results expressed as nanograms of HDL per milligram of tissue wet weight (B). Data represent the mean ± SEM from two independent experiments. Statistical significance is denoted as *$P < 0.05$; n = 9 mice/group for the 1 h and 24 h, and 4 mice/group for the 48 h time point.

indicated that in the m-RCT experiment the initial dose of histamine must have stimulated the passage of HDL through the skin over a period of 24 h and that the second dose must have exerted an additive effect further increasing the availability of HDL particles in the skin site. Thus, the two doses must have triggered two similar 24 h periods during which an enhanced flow of endogenous (unlabeled) HDL through the treated skin site provided twice the conditions for a more efficient RCT initiation from tissue macrophages. These results are compatible with a moderate nonsignificant increase of m-RCT observed with one histamine dose and the more robust stimulatory effect observed with the two doses.

Serotonin and bradykinin stimulate HDL uptake by skin and promote RCT from skin macrophages to feces

To further test the hypothesis that the histamine-induced increase in the influx of HDL into the skin was due to increased vascular permeability, we repeated the above experiment using two other natural vasoactive compounds. We selected serotonin and bradykinin, which, like histamine, are endogenous inflammatory mediators that have been demonstrated to also rapidly increase vascular permeability in rodents (15, 21). Thus, mice received subcutaneous injections of either serotonin (500 μg/kg), bradykinin (500 μg/kg), or vehicle, and the influx of intravenously injected [^{3}H]HDL to the treated skin sites was measured at 1 h and 24 h. The results indicated that, comparable to histamine, both serotonin and bradykinin stimulated within 1 h the influx of [^{3}H]HDL to the injected skin site, whereas after 24 h of injection the [^{3}H]HDL content in the skin decreased to the level of the control group (**Fig. 4A**). Neither serotonin nor bradykinin affected the kinetics of the circulating pool of [^{3}H]HDL (Fig. 4A, inset). Next, we evaluated the effect of subcutaneous administration of serotonin and bradykinin on m-RCT to feces. For this purpose, either compound was subcutaneous injected immediately after the injection of the [^{3}H] cholesterol-labeled macrophages, and the transfer of the ^{3}H-tracer to feces was determined. Like histamine, both compounds were administered twice, 24 h apart, and feces were collected over 48 h. As shown in Fig. 4B, C, administration of either compound stimulated significantly the excretion of [^{3}H]cholesterol and the appearance of the ^{3}H-tracer in the bile acid fraction in feces, so the total fecal ^{3}H-radioactivity significantly increased. Altogether, the data revealed that, besides histamine, other physiological vasoactive compounds also have the potential to increase

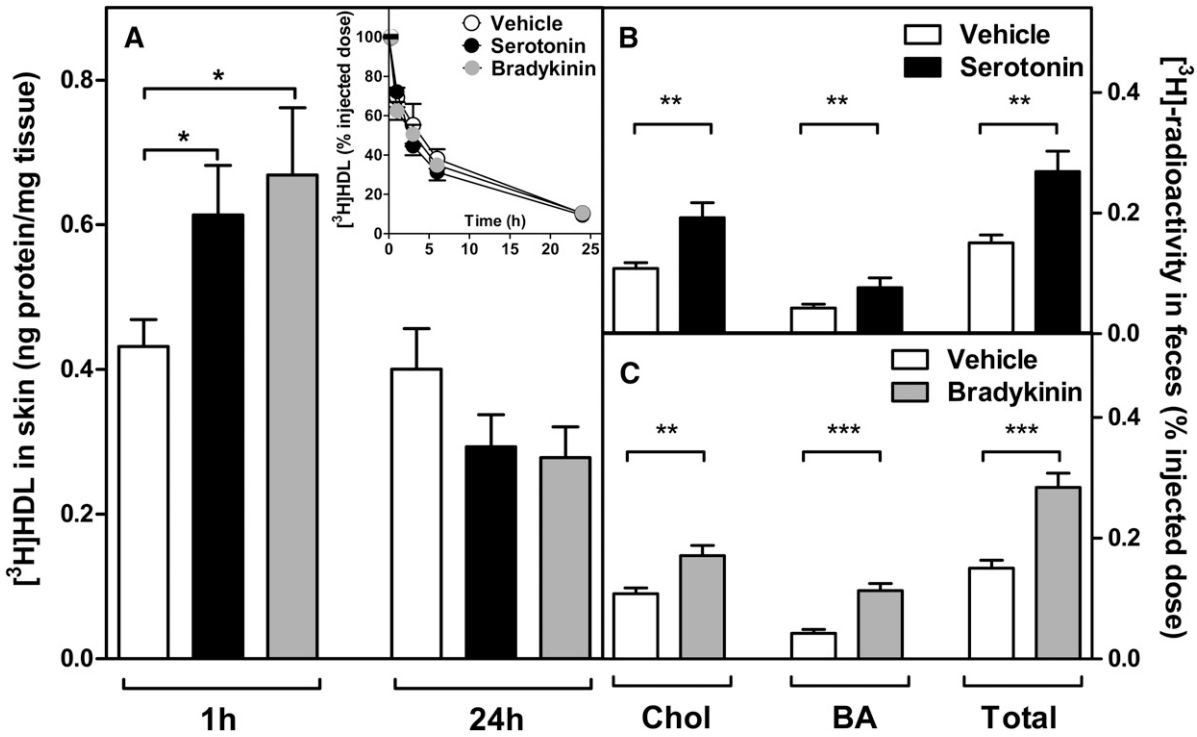

Fig. 4. Serotonin and bradykinin increase the influx of HDL to skin and stimulate m-RCT from skin to feces. The influx of HDL to skin and decay curves for the tracer in plasma were evaluated up to 24 h in mice that received subcutaneous injections of serotonin (500 μg/kg), bradykinin (500 μg/kg), or vehicle alone immediately followed by intravenous injection of a labeled HDL preparation, as described in Fig. 3. Samples of skin were dissected from the site of subcutaneous injection at 1 h and 24 h, and blood samples analyzed for the decay curves (inset) were collected at similar time points as described in Fig. 3. Radioactivity was measured in the tissue extracts, and the results expressed as nanograms of HDL per milligram of tissue wet weight (A). To evaluate m-RCT, mice received subcutaneous injection of [^{3}H] cholesterol-labeled J774 macrophage foam cells immediately followed by subcutaneous injection of serotonin (500 μg/kg), bradykinin (500 μg/kg), or vehicle alone to the dorsal skin site. Treatments with serotonin and bradykinin were repeated 24 h after the initial injection to the respective group of mice. The rate of m-RCT from skin to feces ([^{3}H]cholesterol + [^{3}H]bile acids) was determined, as described in Fig. 1, in serotonin-treated (B) and bradykinin-treated (C) groups. Data represent the mean ± SEM from two to three independent experiments. Statistical significance is denoted as * $P < 0.05$, ** $P < 0.01$, *** $P < 0.001$; n = 10–12 mice/group.

the skin-originated m-RCT resulting from an increase in the permeability to HDL of the vascular bed surrounding the macrophages.

Vasoactive compounds do not affect cholesterol efflux from cultured macrophages

We next evaluated the potential effects of the vasoactive compounds on the gene expression of cholesterol efflux transporters in macrophages and the ability of cultured J774 macrophage foam cells to efflux cholesterol to mouse serum. To generate preconditioned cells, we incubated the J774 macrophages with decreasing concentrations of the compounds for up to 3 h (see Materials and Methods) but did not find any changes in the gene expression levels of the ABCA1, ABCG1, or SR-BI transporter (**Fig. 5A**). Of the two histamine receptor antagonists, the H2R antagonist ranitidine induced overexpression of macrophage ABCA1 relative to the control cells (1.51 ± 0.1 vs. 1.0 ± 0.1, $P = 0.03$), which may partially explain its less marked effect in blocking the stimulatory effect of histamine on m-RCT (see Fig. 2). Importantly, the efficiency of the preconditioned macrophages to efflux cholesterol was not affected when the cells were further incubated for 3 h in mouse serum-containing medium (Fig. 5B). Analysis of serum lipids in mice treated with histamine and histamine receptor antagonists indicated that administration of the various compounds did not affect circulating lipid levels, particularly HDL-cholesterol, indicating that the treatments had not modified the cholesterol efflux capacity of the serum (**Table 1**). Neither did serotonin influence serum lipids; however, bradykinin treatment decreased triglyceride levels without having any effect on HDL-cholesterol levels (**Table 2**). Altogether, these results provided strong supportive evidence for the claim that a local increase in the vascular permeability inducing enhanced entry of HDL particles into skin, rather than modification of the intrinsic efficiency of the macrophage cholesterol efflux pathways, was the driving mechanism promoting m-RCT in vivo when skin was treated with the vasoactive compounds.

Histamine administration to apoA-I-deficient mice increases m-RCT from skin to feces in the presence of exogenous HDL

Because the stimulatory effect of increasing vascular permeability on m-RCT depended on the increased passage of HDL particles to the skin site where the macrophage foam cells were present, it seemed very likely that under conditions of low serum HDL levels the effect of the vasoactive compounds on m-RCT would be reduced. We predicted that in this experimental setting a transient enrichment of serum with exogenous HDL would result in enhanced passage of HDL through the leaky endothelium to the skin site, thereby stimulating the m-RCT rate. We tested these predictions in apoA-I-KO mice, which present 2-fold lower levels of HDL-cholesterol relative to the wild-type mice (**Table 3**). The basic m-RCT protocol used in this work was applied with the exception that the mice received an intravenous injection of HDL isolated

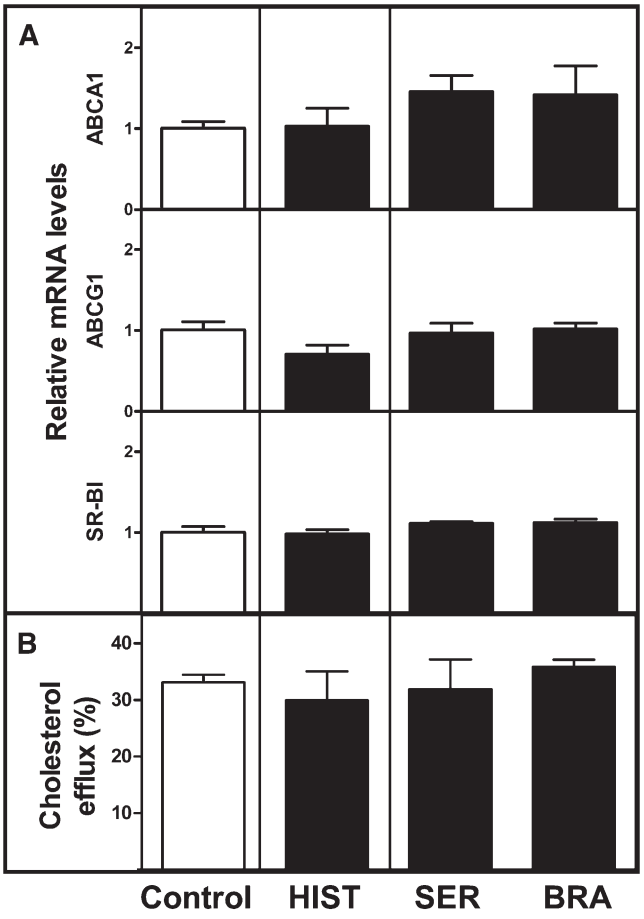

Fig. 5. Vasoactive compounds do not modify gene expression of cholesterol efflux transporters nor cholesterol efflux from cultured J774 macrophages. J774 macrophage foam cells were incubated in media containing decreasing concentrations of histamine (HIST), serotonin (SER), or bradykinin (BRA) for various intervals of time, up to 3 h (preconditioned macrophages). The concentration of each compound in media was set initially at the respective injected concentration, as shown in Figs. 1 and 4, and was progressively reduced within intervals of 10 min, to achieve a final 100-fold reduction at 30 min of incubation, which was prolonged until 3 h. Macrophages incubated in the absence of vasoactive compounds acted as control. The relative mRNA expression of ABCA1, ABCG1, and SR-BI genes was determined by RT-PCR in the preconditioned macrophages derived from triplicate wells. The signal of control macrophages was set at a normalized value of 1 arbitrary unit, and GAPDH was used as internal control (A). Cholesterol efflux from [^{3}H]cholesterol-labeled J774 macrophage foam cells to mouse serum (2.5% in medium) was assessed after the preconditioning incubation step of the cells in the presence of the vasoactive compounds at their final concentrations, as described above. Nonpreconditioned macrophages incubated in the absence of vasoactive compounds and in the presence of serum alone acted as control. Fractional cholesterol efflux (%) was expressed as $dpm_{medium} / (dpm_{cells} + dpm_{medium}) \times 100$ (B). All data represent the mean ± SEM from four replicate wells.

from wild-type mice immediately after the initial subcutaneous injection of histamine. The single dose of HDL had only a short-lasting effect on the basal low HDL levels, and, accordingly, after 48 h the plasma lipids were not changed (Table 3). Measurement of the transfer of macrophage-derived cholesterol to feces indicated that administration of merely histamine to apoA-I-KO mice

TABLE 1. Serum lipids in wild-type mice treated with histamine and histamine receptor antagonists

Lipid (mM)	Vehicle	Histamine	H1R Antagonist	H2R Antagonist	H1R+H2R Antagonist
Total cholesterol	2.5 ± 0.13	2.4 ± 0.13	2.7 ± 0.22	2.5 ± 0.301	2.6 ± 0.25
HDL-cholesterol	1.9 ± 0.05	1.8 ± 0.11	2.0 ± 0.20	1.8 ± 0.29	2.0 ± 0.21
Triglycerides	1.6 ± 0.09	1.4 ± 0.11	1.6 ± 0.08	1.5 ± 0.13	1.4 ± 0.06

Mice were treated with histamine (250 μg/kg), the H1R antagonist pyrilamine (20 mg/kg), the H2R antagonist ranitidine (20 mg/kg), or vehicle alone. The data presented correspond to serum obtained at the final time point (48 h) of the experiment shown in Fig. 2. Data represent the mean ± SEM.

resulted in a slight, nonsignificant increase of m-RCT (**Fig. 6**), which may have been caused by the low residual levels of apoA-I-deficient HDL in the serum of these mice. Neither did intravenous administration of HDL alone (i.e., without histamine) produce any effect on m-RCT. However, when exogenous HDL was administered together with histamine, the m-RCT rate increased significantly. Altogether, these data showed that, on a low-HDL background, increase of circulating HDL levels and triggering of local vascular leakage were both required to enhance passage of plasma HDL into the skin and accelerate the initiation of m-RCT from the subcutaneously located macrophages.

Histamine administration does not modify m-RCT from skin to feces in the presence of high levels of circulating non-HDL lipoproteins

We speculated that if apoB lipoproteins, instead of HDL, were the predominant class of lipoproteins in the mouse plasma, the beneficial effect on m-RCT of increasing the vascular permeability could be challenged. Thus, following our basic protocol, we evaluated the effect of histamine on the rate of m-RCT from skin in the atherosclerosis-prone LDLr-KO mice, which exhibit normal HDL levels but 10-fold higher levels of non-HDL (apoB lipoproteins) relative to the wild-type (**Table 4**). We found that, under such hypercholesterolemic background, histamine did not increase the transfer of macrophage-derived radioactivity to serum, liver, or feces (**Fig. 7**). However, the magnitude of the recovered macrophage-derived radioactivity reflected high transfer rates to serum, and particularly to the nonHDL fraction (Fig. 7A), which accounted for ∼80% of the total radioactivity in the serum of both vehicle- and histamine-treated mice. The high levels of the ^{3}H-tracer recovered in feces suggested that LDLr-KO mice might exhibit high m-RCT rates already under basal conditions, that is, ∼4-fold higher total radioactivity in feces (0.45% of injected dose) relative to the wild-type mice (0.11% in Fig. 1C, and 0.10% in Fig. 4B, C). The finding that histamine did not have any further effect on such apparently accelerated basal m-RCT rate in LDLr-KO mice rather suggested that histamine and hypercholesterolemia may have shared a common stimulatory mechanism, such as the vascular leakage, which has been, indeed, found to occur in hypercholesterolemic mice (22, 23).

TABLE 2. Serum lipids in wild-type mice treated with serotonin or bradykinin

Lipid (mM)	Vehicle	Serotonin	Bradykinin
Total cholesterol	2.8 ± 0.21	2.8 ± 0.12	2.7 ± 0.19
HDL-cholesterol	1.8 ± 0.08	1.8 ± 0.13	1.8 ± 0.29
Triglycerides	1.6 ± 0.08	1.4 ± 0.10	1.0[a] ± 0.12

Mice received subcutaneous injections of serotonin (500 μg/kg), bradykinin (500 μg/kg), or vehicle alone. The data presented correspond to serum obtained at the final time point (48 h) of the experiments shown in Fig. 4B, C. Data represent the mean ± SEM. Statistical significance relative to the vehicle group is denoted as [a] $P <$ 0.001.

Endogenous histamine released from activated mast cells increases m-RCT from skin

Mast cells are inflammatory cells, which, when activated to degranulate, release histamine and several other vasoactive compounds in vivo (24). Because mast cells are the major source of histamine in the subcutaneous layer of skin (25), we evaluated whether their local activation could influence the rate of m-RCT. For this purpose, m-RCT was measured following our basic protocol in wild-type mice that had received subcutaneous injection of the noncytotoxic mast cell-specific degranulating compound 48/80 1 h before the [^{3}H]cholesterol-labeled J774 macrophages were injected into the same area of skin. We found that 48/80 effectively induced mast cell activation in the skin, which, when compared with vehicle, resulted in exocytosis of the cytoplasmic granules at the site of injection (**Fig. 8A**, right, upper, and lower panels, respectively) and could be quantitatively assessed by determining the numbers of degranulated mast cells at the injection site (Fig. 8A, left, upper panel). The observed reduction of histamine content in the tissue site in which the mast cells had been activated agrees well with the known diffusion and rapid escape of the released histamine from the mast cell activation site (Fig. 8A, bottom left). Importantly, we found that a single injection of 48/80 that induced degranulation of ∼70% mast cells in the treated skin area was sufficient to increase the m-RCT rate (Fig. 8B). Treatment of mice with 48/80 did not modify serum lipids (**Table 5**), nor did addition of 48/80 to cultured [^{3}H]cholesterol-labeled J774 macrophage foam cells affect the ability of the cells to efflux cholesterol to mouse serum (Fig. 8B, inset). These data demonstrate that activation of skin mast cells with ensuing release of histamine and other vasoactive compounds is capable of stimulating the basal rate of RCT from nearby macrophage foam cells in vivo.

DISCUSSION

A given concentration of lipoprotein particles in the interstitial fluid results from the balance determined by the

TABLE 3. Serum lipids in apoA-I-KO mice treated with histamine and/or HDL

Lipid (mM)	Vehicle	HDL	Histamine	Histamine+HDL
Total cholesterol	1.2 ± 0.09	0.8 ± 0.10	1.0 ± 0.12	1.1 ± 0.06
HDL-cholesterol	0.8 ± 0.13	0.6 ± 0.08	0.6 ± 0.06	0.6 ± 0.06
Triglycerides	1.1 ± 0.18	1.0 ± 0.14	1.0 ± 0.18	1.1 ± 0.18

Mice received subcutaneous injection of histamine (250 μg/kg), intravenous injection of HDL (4–6 mg protein/kg), or both. Mice that received vehicle alone acted as control group. The data presented correspond to serum obtained at the final time point (48 h) of the experiment shown in Fig. 6. Data represent the mean ± SEM.

ratio of particles entering via the capillaries and those removed via the lymphatic vasculature (26, 27). Although it is likely that modification of the vascular permeability, similar to variations in the lymphatic flow (13, 14), may locally modify the concentration of HDL particles in the interstitial fluid and so influence the initiation of RCT from peripheral macrophages, a direct role for an increase in vascular permeability as a regulator of m-RCT has not been experimentally proven before. Here we evaluated the RCT rate from cholesterol-labeled macrophages injected into the highly vascularized subcutaneous skin layer of mice in which influx of circulating HDL was enhanced by treatment with various vasoactive compounds. Because skin also contains various types of cells secreting vasoactive compounds, notably the mast cells, skin was considered to be a suitable tissue where HDL concentration could also be raised by naturally occurring endogenous compounds capable of increasing the vascular permeability. We demonstrated that sole administration of histamine, serotonin, or bradykinin, each capable of increasing vascular permeability facilitated the entry to the treated skin of circulating HDL particles, the main lipoprotein component in mouse plasma. Importantly, this effect was sufficient to increase the rate of RCT originating in vivo from macrophages located within the treated skin area. Because none of the vasoactive compounds studied here affected the serum HDL levels or the rate of cholesterol efflux from the cultured J774 macrophages, the stimulation of m-RCT in vivo must have been due to increased entry of circulating HDL into the treated skin, rather than due to an increased cholesterol efflux potential of the cholesterol acceptors or donors per se. These findings support a novel independent role for the rate of the passage of plasma HDL to the interstitial fluids in regulating m-RCT rate from peripheral tissues and, accordingly, the cholesterol content of macrophages in these body compartments.

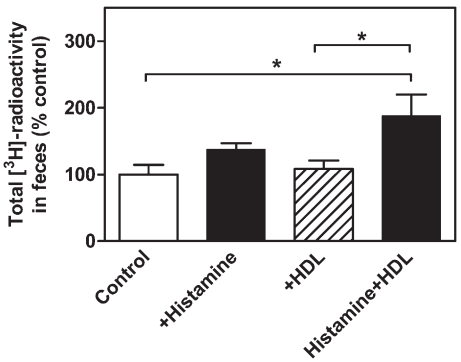

Fig. 6. HDL administration to apoA-I-KO mice restores the ability of histamine to increase m-RCT from skin to feces. [^{3}H]cholesterol-labeled J774 macrophage foam cells were injected into the dorsal skin of apoA-I-KO mice, as described in Fig. 1. Immediately thereafter, mice received subcutaneous histamine injection into an adjacent skin site, followed by a subsequent intravenous injection of isolated mouse HDL or vehicle. The transfer of macrophage-derived [^{3}H]cholesterol to feces was determined by measuring the radioactivity in the feces collected within 48 h. Excretion of the [^{3}H]tracer in feces corresponds to the [^{3}H]cholesterol + [^{3}H]bile acid fractions. Data represent the mean ± SEM from two independent experiments and were normalized as percent of control (vehicle). Mean value obtained in the vehicle group was 0.24 ± 0.04, and it was set as 100%. Statistical significance is denoted as * $P < 0.05$; n = 4–5 mice/group.

The passage of lipoproteins across the normal intact endothelium is a regulated process that occurs mainly by transcellular routes (28), while the ultrafiltration of circulating lipoproteins at sites of endothelial activation where vascular permeability is increased has been found to be a paracellular process that occurs at the site of gaps between the endothelial cells (29). It has been established that inflammatory mediators such as histamine, bradykinin, serotonin, and other vasoactive compounds, upon binding to their receptors on endothelial cells, disrupt the organization of the interendothelial junctions, thus leading to opening of the endothelial barrier (30). The size of the gaps can be considerable; for example, it was reported that substance P may induce gaps in the interendothelial junctions of endothelial cells in vessels of the rat trachea that range from 100 to 400 nm and have a half-life of ~1.9 min (31). Histamine, a vasoactive compound primarily released by activated mast cells, and in small quantities also by other cells, such as the endothelial cells themselves, is the most studied compound in in vitro models of vascular permeability. Importantly, the increase of vascular permeability induced by histamine has resulted in immediate extravasation of LDL from plasma to skin in rats and hamsters (15, 32). The rapid extravascular accumulation of LDL most likely results from the sieving of lipoproteins

TABLE 4. Serum lipids in LDLr-KO mice treated with histamine

Lipid (mM)	Vehicle	Histamine
Total cholesterol	11.8 ± 1.6	9.9 ± 0.4
HDL-cholesterol	1.6 ± 0.3	1.7 ± 0.2
Triglycerides	2.5 ± 0.2	1.8 ± 0.2

Mice received subcutaneous injection of histamine (250 μg/kg) or vehicle. The data presented correspond to serum obtained at the final time point (48 h) of the experiment shown in Fig. 7. Data represent the mean ± SEM.

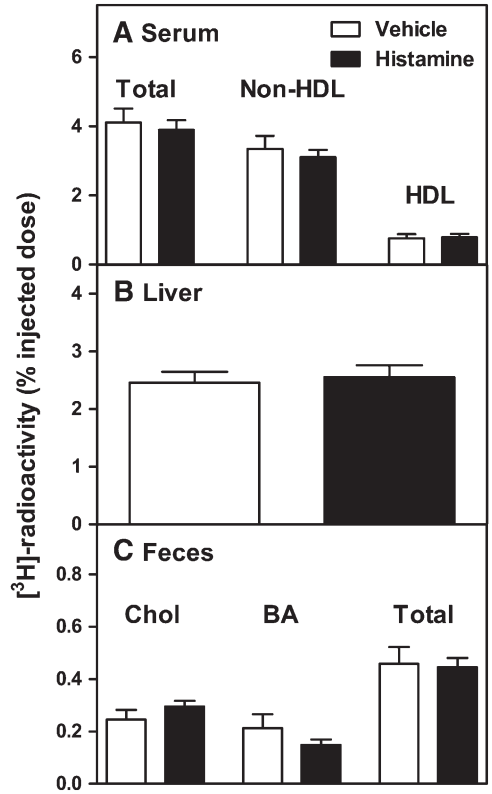

Fig. 7. Histamine does not stimulate in vivo m-RCT in LDLr-KO mice. LDLr-KO mice received subcutaneous injection of [^{3}H]cholesterol-labeled foam cells followed by two subcutaneous injections of histamine (250 μg/kg) or vehicle. The transfer of macrophage-derived [^{3}H]cholesterol from the skin to serum and to the non-HDL and HDL fraction (A), to liver (B), and to feces (C) was determined after 48 h. N = 7 mice/group.

through water pores of ~22 nm in radius, up to the size of LDL (32). Such transient increase in endothelial permeability induced by histamine may be prolonged by thrombin via a mechanism that involves modulation of the intracellular levels of calcium ions, as it was shown in human endothelial cell monolayers (33).

Because the permeability-enhancing effect of histamine is rapid and transitory, we administered two subsequent doses, which, by opening the endothelial gaps twice, facilitated the influx of sufficient amounts of circulating HDL into the skin and increased m-RCT rate over a 48 h period. Under these experimental conditions, the stimulatory effect of histamine on m-RCT appeared to be mediated mainly by the H1R, with the H2R exerting a small additive effect. Consistent with our findings, activation of H1R, rather than H2R, has been found to enhance vascular permeability for endogenous LDL in cholesterol-fed apoE$^{-/-}$ mice without altering the plasma lipoprotein levels (34). It has been also shown that histamine increases the passage of LDL through monolayers of human arterial endothelial cells, having its peak at 2 h but rapidly decreasing to the control level within 4–6 h, and, moreover, that this effect can be blocked by the H1R antagonist pyrilamine, rather than by the H2R antagonist cimetidine (35). The requirement of two doses of histamine for the m-RCT response could also mean that the second dose of histamine had an additive effect, which was qualitatively different from that achieved with the initial dose (e.g., on the lymph flow). Indeed, complex and even opposite effects of histamine on the lymphatic function have been reported. Thus, histamine appeared to stimulate the lymphatic vessel contractile activity (36), to act as an endothelium-derived relaxing factor in mesenteric lymphatic vessels (37), or to disrupt the integrity of the barrier function of lymphatic endothelial cells, thereby potentiating leakage of solutes from lymph back to the interstitial space (38). Whether the second dose of histamine had also activated the lymphatic SR-BI transporter recently found to regulate the entry of HDL into the lymphatic vessels (14) remains unknown.

In the present studies, we use wild-type mice fed a standard chow diet as our experimental model. However, in contrast to mice, which are HDL animals, in humans most of the cholesterol is transported in LDL, and, moreover, severe hypercholesterolemia due to increased LDL levels is associated with accumulation of cholesterol in peripheral tissues, particularly in the intimal layer of arteries generating atherosclerotic lesions and also in the skin generating xanthomas (39). In this context, it is of particular relevance that the genetic absence of apoA-I in humans also results in the formation of skin xanthomas, so revealing a critical role of this apolipoprotein in the regulation of skin cholesterol balance (40). Notably, the present results support the view that an increased passage of apoA-I-containing HDL to the interstitial fluid of the skin is capable of locally accelerating m-RCT from cholesterol-loaded cells and so potentially able to decrease the accumulation of cholesterol found in skin xanthomas. In an attempt to mimic the human hypercholesterolemic phenotype, we also evaluated the effect of increasing vascular permeability in the LDLr-KO mouse, which exhibits high non-HDL/HDL ratio and is considered an animal model of familial hypercholesterolemia (FH) (41). Surprisingly, the basal rate of m-RCT already appeared to be increased in the untreated LDLr-KO mice relative to the untreated wild-type mice (compare the vehicle groups in Fig. 7C and Figs. 1C and 4B, C) and treatment with histamine failed to have any further additive effect on the basal rate in the KO mice. Because hypercholesterolemia weakens the endothelial junctions and increases vascular permeability in mice (22, 23), histamine may have failed when acting on an endothelium already leaky. To our best knowledge, no published data on the efficiency of m-RCT in LDLr-KO mice are available. Thus, we can only speculate that high m-RCT rates in the LDLr-deficient mice (Fig. 7C) might have been caused by an enhanced passage of plasma HDL through the skin followed by an alternative m-RCT route that includes transfer of cholesterol to LDL and uptake of the cholesterol-enriched LDL by the hepatic LRP receptor (42). In addition, efflux of macrophage cholesterol to LDL could predominate when its concentration exceeds that of HDL (43). The induction of high rates of m-RCT in a mouse model of FH observed in the present study and also in cholesterol-fed wild-type mice (44) would seem to challenge the concept that the rate of m-RCT predicts atherosclerosis susceptibility, at least in the mouse.

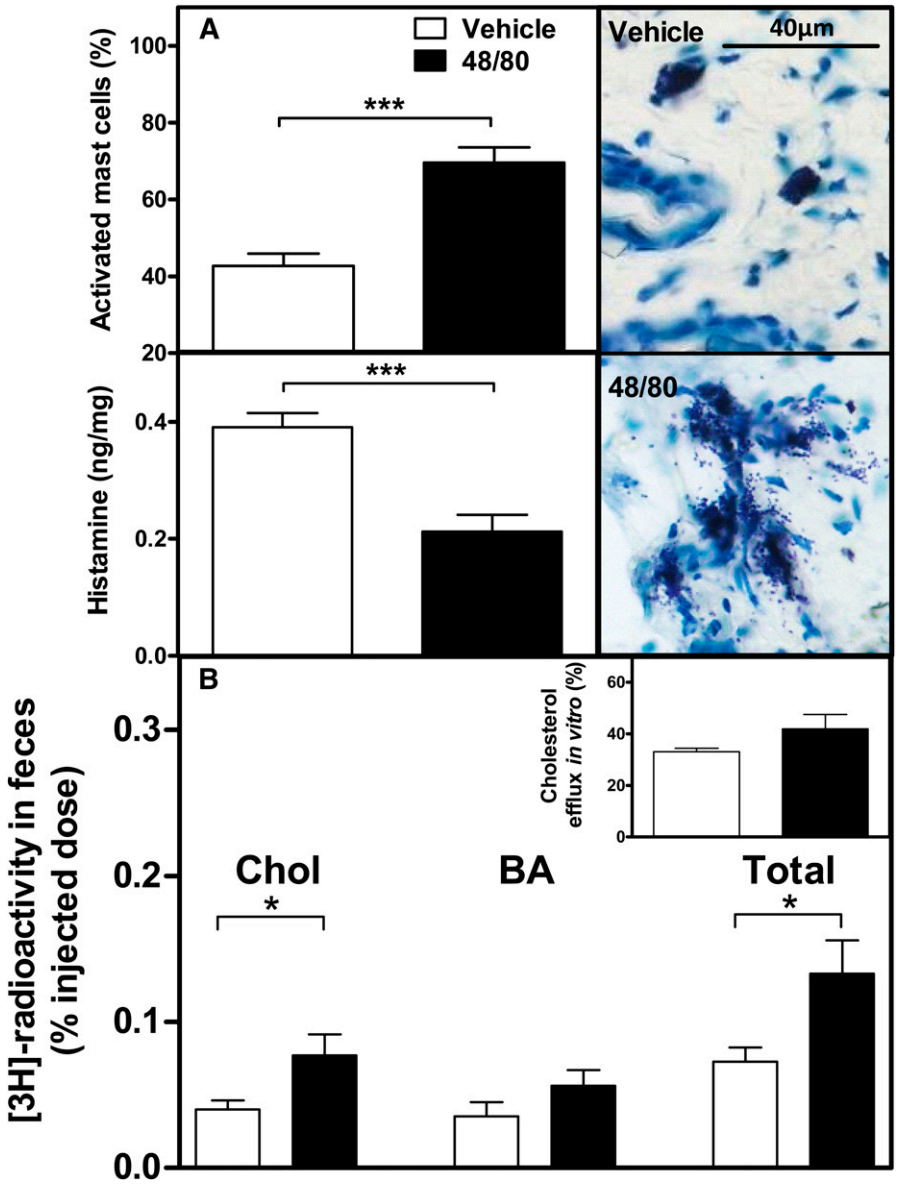

Fig. 8. Treatment with 48/80 activates skin mast cells and stimulates m-RCT from skin. Mast cells in the skin were activated to degranulate by subcutaneous injection of 48/80 (2.5 mg/kg). After 48 h of injection, a piece of skin was cut from the injection site and snap-frozen in liquid nitrogen. The proportion of activated mast cells from the total population of mast cells in the skin site (A, top left) was determined in 0.1% Toluidine Blue-stained histological samples. Mast cells were classified as resting (A, top right) or degranulated (A, bottom right) by the absence or presence, respectively, of extracellular granules present in the immediate vicinity of a mast cell. One hour after the injection of 48/80 (2.5 mg/kg), mice were euthanized and a piece of skin (area of 1 cm^2) was dissected from the injection site. Histamine content was determined fluorometrically from skin samples, and the results were expressed as nanograms of histamine per weight of skin (A, bottom left). Mice received subcutaneous injection of [^{3}H]cholesterol-labeled J774 foam cells immediately followed by subcutaneous injection of 48/80 or vehicle alone. The transfer of macrophage-derived [^{3}H]cholesterol to feces was determined by measuring the radioactivity in the feces collected within 48 h. Excretion of the [^{3}H]tracer in feces corresponds to the [^{3}H]cholesterol + [^{3}H]bile acid fractions (B). Statistical significance are denoted as * $P < 0.05$, *** $P < 0.001$; n = 5–8 mice/group. Cholesterol efflux from cultured [^{3}H]cholesterol-labeled J774 macrophage foam cells (see insert in B) to mouse serum (2.5% in medium) was assessed in the presence of 48/80 (50 µg/ml in medium). Fractional cholesterol efflux (%) was expressed as $dpm_{medium} / (dpm_{cells} + dpm_{medium}) \times 100$.

We finally tested our permeability hypothesis in a model of local inflammation by activating mast cells in the skin of wild-type mice to degranulate and to secrete a wide cocktail of vasoactive mediators, notably histamine, serotonin, leukotrienes, and prostaglandins (25, 45). Of note, mast cells are the only resident cells in the rodent skin tissue, which upon activation acutely secrete preformed fully active neutral serine proteases (46). The

TABLE 5. Serum lipids in wild-type mice treated with compound 48/80

Lipid (mM)	Vehicle	48/80
Total cholesterol	2.3 ± 0.15	2.5 ± 0.10
HDL-cholesterol	1.4 ± 0.19	1.4 ± 0.16
Triglycerides	1.1 ± 0.05	1.0 ± 0.10

Mice received subcutaneous injection of 48/80 (2.5 mg/kg) or vehicle alone. The data presented correspond to serum obtained at the final time point (48 h) of the experiment shown in Fig. 8B. Data represent the mean ± SEM.

mast cell-derived chymases, particularly the mouse mast cell protease-4 (mMCP-4), are capable of degrading mouse HDL in the extravascular fluids of tissues in which mast cells have been activated, as has been observed during systemic mast cell activation in a mouse model of systemic anaphylaxis (47). When considering the above background information, it is likely that the actual impact of mast cell activation on HDL functionality in vivo will depend on the balance between the vasoactive and proteolytic effects, which may vary when tested in different experimental settings. We can infer that the present findings disclosed a scenario in which an acute endogenous release of a mixture of vasoactive compounds increasing the influx of HDL to the skin site was capable of overriding the inhibitory effect of the coreleased proteases on an expanded interstitial pool of HDL. It is likely that the transient and highly local proteolytic effect of the granule-bound proteases is challenged by their rapid phagocytosis by neighboring cells, such as fibroblasts, endothelial cells, and particularly macrophages at the skin site artificially enriched with these cells (48, 49).

The present study is the first to link an increased endothelial permeability with increased rates of RCT from peripheral tissue macrophages. It was recently reported that the function of lymphatic vessels clearing HDL from skin remains as the dominant conduits for m-RCT also in tissues surrounding an implanted tumor in mice characterized by increased vascular permeability (13). A more detailed characterization of the relative roles played by the vascular permeability and lymphatic drainage regulating coordinately the inward and outward flow of HDL on the RCT rate deserves further investigation. Finally, we envision that the proatherogenic effect of increased vascular permeability that is associated with increased influx of LDL (15) is counteracted by simultaneously increased influx of HDL, particularly of the functionally highly competent and very small-sized HDL particles, such as preβ_1-HDL. Because an increase in the vascular permeability will induce an increased passage of both LDL and HDL, and we lack pharmacological means of selectively preventing the passage of LDL, maintaining the proper balance between the proatherogenic LDL and the antiatherogenic HDL in the circulation remains the main clinical strategy when aiming to reduce the formation of macrophage foam cells or trying to accelerate their regression.

The authors thank Mari Jokinen for her excellent technical assistance.

REFERENCES

1. Levick, J. R., and C. C. Michel. 2010. Microvascular fluid exchange and the revised Starling principle. *Cardiovasc. Res.* **87:** 198–210.
2. Stender, S., and D. B. Zilversmit. 1981. Transfer of plasma lipoprotein components and of plasma proteins into aortas of cholesterol-fed rabbits. Molecular size as a determinant of plasma lipoprotein influx. *Arteriosclerosis.* **1:** 38–49.
3. Nielsen, L. B. 1996. Transfer of low density lipoprotein into the arterial wall and risk of atherosclerosis. *Atherosclerosis.* **123:** 1–15.
4. Lee-Rueckert, M., F. Blanco-Vaca, P. T. Kovanen, and J. C. Escola-Gil. 2013. The role of the gut in reverse cholesterol transport – focus on the enterocyte. *Prog. Lipid Res.* **52:** 317–328.
5. Cuchel, M., and D. J. Rader. 2006. Macrophage reverse cholesterol transport: key to the regression of atherosclerosis? *Circulation.* **113:** 2548–2555.
6. Rader, D. J., and A. R. Tall. 2012. The not-so-simple HDL story: is it time to revise the HDL cholesterol hypothesis? *Nat. Med.* **18:** 1344–1346.
7. Nissen, S. E., T. Tsunoda, E. M. Tuzcu, P. Schoenhagen, C. J. Cooper, M. Yasin, G. M. Eaton, M. A. Lauer, W. S. Sheldon, C. L. Grines, et al. 2003. Effect of recombinant ApoA-I Milano on coronary atherosclerosis in patients with acute coronary syndromes: a randomized controlled trial. *J. Am. Med. Assoc.* **290:** 2292–2300.
8. Tardif, J. C., J. Gregoire, P. L. L'Allier, R. Ibrahim, J. Lesperance, T. M. Heinonen, S. Kouz, C. Berry, R. Basser, M. A. Lavoie, et al. 2007. Effects of reconstituted high-density lipoprotein infusions on coronary atherosclerosis: a randomized controlled trial. *J. Am. Med. Assoc.* **297:** 1675–1682.
9. Lutgers, H. L., R. Graaff, R. de Vries, A. J. Smit, and R. P. Dullaart. 2010. Carotid artery intima media thickness associates with skin autofluoresence in non-diabetic subjects without clinically manifest cardiovascular disease. *Eur. J. Clin. Invest.* **40:** 812–817.
10. Stein, J. H., W. S. Tzou, J. M. DeCara, A. T. Hirsch, E. R. Mohler III, P. Ouyang, G. L. Pearce, and M. H. Davidson. 2008. Usefulness of increased skin cholesterol to identify individuals at increased cardiovascular risk (from the Predictor of Advanced Subclinical Atherosclerosis study). *Am. J. Cardiol.* **101:** 986–991.
11. Tzou, W. S., M. E. Mays, C. E. Korcarz, S. E. Aeschlimann, and J. H. Stein. 2005. Skin cholesterol content identifies increased carotid intima-media thickness in asymptomatic adults. *Am. Heart J.* **150:** 1135–1139.
12. Rapp, J. H., W. E. Connor, D. S. Lin, T. Inahara, and J. M. Porter. 1983. Lipids of human atherosclerotic plaques and xanthomas: clues to the mechanism of plaque progression. *J. Lipid Res.* **24:** 1329–1335.
13. Martel, C., W. Li, B. Fulp, A. M. Platt, E. L. Gautier, M. Westerterp, R. Bittman, A. R. Tall, S. H. Chen, M. J. Thomas, et al. 2013. Lymphatic vasculature mediates macrophage reverse cholesterol transport in mice. *J. Clin. Invest.* **123:** 1571–1579.
14. Lim, H. Y., C. H. Thiam, K. P. Yeo, R. Bisoendial, C. S. Hii, K. C. McGrath, K. W. Tan, A. Heather, J. S. Alexander, and V. Angeli. 2013. Lymphatic vessels are essential for the removal of cholesterol from peripheral tissues by SR-BI-mediated transport of HDL. *Cell Metab.* **17:** 671–684.
15. Ma, H., and P. T. Kovanen. 1997. Degranulation of cutaneous mast cells induces transendothelial transport and local accumulation of plasma LDL in rat skin in vivo. *J. Lipid Res.* **38:** 1877–1887.
16. Manaenko, A., H. Chen, J. Kammer, J. H. Zhang, and J. Tang. 2011. Comparison Evans Blue injection routes: intravenous versus intraperitoneal, for measurement of blood-brain barrier in a mice hemorrhage model. *J. Neurosci. Methods.* **195:** 206–210.
17. Shore, P. A., A. Burkhalter, and V. H. Cohn, Jr. 1959. A method for the fluorometric assay of histamine in tissues. *J. Pharmacol. Exp. Ther.* **127:** 182–186.
18. Laine, P., M. Kaartinen, A. Penttilä, P. Panula, T. Paavonen, and P. T. Kovanen. 1999. Association between myocardial infarction and the mast cells in the adventitia of the infarct-related coronary artery. *Circulation.* **99:** 361–369.
19. Bolton, A. E., and W. M. Hunter. 1973. The labelling of proteins to high specific radioactivities by conjugation to a 125-I-containing acylating agent. *Biochem. J.* **133:** 529–539.
20. Silvennoinen, R., J. C. Escola-Gil, J. Julve, N. Rotllan, G. Llaverias, J. Metso, A. F. Valledor, J. He, L. Yu, M. Jauhiainen, et al. 2012. Acute psychological stress accelerates reverse cholesterol transport

via corticosterone-dependent inhibition of intestinal cholesterol absorption. *Circ. Res.* **111:** 1459–1469.
21. Colditz, I. G. 1991. The induction of plasma leakage in skin by histamine, bradykinin, activated complement, platelet-activating factor and serotonin. *Immunol. Cell Biol.* **69:** 215–219.
22. Phinikaridou, A., M. E. Andia, G. Passacquale, A. Ferro, and R. M. Botnar. 2013. Noninvasive MRI monitoring of the effect of interventions on endothelial permeability in murine atherosclerosis using an albumin-binding contrast agent. *J. Am. Heart Assoc.* **2:** e000402.
23. Tomizawa, A., I. Ishii, Z. Zhelev, I. Aoki, S. Shibata, M. Kitada, and R. Bakalova. 2011. Carbamoyl-PROXYL-enhanced MRI detects very small disruptions in brain vascular permeability induced by dietary cholesterol. *Biochim. Biophys. Acta.* **1810:** 1309–1316.
24. Kunder, C. A., A. L. St John, and S. N. Abraham. 2011. Mast cell modulation of the vascular and lymphatic endothelium. *Blood.* **118:** 5383–5393.
25. Kovanen, P. T. 2009. Mast cells in atherogenesis: actions and reactions. *Curr. Atheroscler. Rep.* **11:** 214–219.
26. Miller, N. E., C. C. Michel, M. N. Nanjee, W. L. Olszewski, I. P. Miller, M. Hazell, G. Olivecrona, P. Sutton, S. M. Humphreys, and K. N. Frayn. 2011. Secretion of adipokines by human adipose tissue in vivo: partitioning between capillary and lymphatic transport. *Am. J. Physiol. Endocrinol. Metab.* **301:** E659–E667.
27. Miller, N. E., W. L. Olszewski, H. Hattori, I. P. Miller, T. Kujiraoka, T. Oka, T. Iwasaki, and M. N. Nanjee. 2013. Lipoprotein remodeling generates lipid-poor apolipoprotein A-I particles in human interstitial fluid. *Am. J. Physiol. Endocrinol. Metab.* **304:** E321–E328.
28. von Eckardstein, A., and L. Rohrer. 2009. Transendothelial lipoprotein transport and regulation of endothelial permeability and integrity by lipoproteins. *Curr. Opin. Lipidol.* **20:** 197–205.
29. Rutledge, J. C., F. R. Curry, J. F. Lenz, and P. A. Davis. 1990. Low density lipoprotein transport across a microvascular endothelial barrier after permeability is increased. *Circ. Res.* **66:** 486–495.
30. Mehta, D., and A. B. Malik. 2006. Signaling mechanisms regulating endothelial permeability. *Physiol. Rev.* **86:** 279–367.
31. McDonald, D. M., G. Thurston, and P. Baluk. 1999. Endothelial gaps as sites for plasma leakage in inflammation. *Microcirculation.* **6:** 7–22.
32. Rutledge, J. C., F. E. Curry, P. Blanche, and R. M. Krauss. 1995. Solvent drag of LDL across mammalian endothelial barriers with increased permeability. *Am. J. Physiol.* **268:** H1982–H1991.
33. van Nieuw Amerongen, G. P., R. Draijer, M. A. Vermeer, and V. W. van Hinsbergh. 1998. Transient and prolonged increase in endothelial permeability induced by histamine and thrombin: role of protein kinases, calcium, and RhoA. *Circ. Res.* **83:** 1115–1123.
34. Rozenberg, I., S. H. Sluka, L. Rohrer, J. Hofmann, B. Becher, A. Akhmedov, J. Soliz, P. Mocharla, J. Boren, P. Johansen, et al. 2010. Histamine H1 receptor promotes atherosclerotic lesion formation by increasing vascular permeability for low-density lipoproteins. *Arterioscler. Thromb. Vasc. Biol.* **30:** 923–930.
35. Langeler, E. G., I. Snelting-Havinga, and V. W. van Hinsbergh. 1989. Passage of low density lipoproteins through monolayers of human arterial endothelial cells. Effects of vasoactive substances in an in vitro model. *Arteriosclerosis.* **9:** 550–559.
36. Fox, J. L., and P. Y. von der Weid. 2002. Effects of histamine on the contractile and electrical activity in isolated lymphatic vessels of the guinea-pig mesentery. *Br. J. Pharmacol.* **136:** 1210–1218.
37. Nizamutdinova, I. T., D. Maejima, T. Nagai, E. Bridenbaugh, S. Thangaswamy, V. Chatterjee, C. J. Meininger, and A. A. Gashev. 2014. Involvement of histamine in endothelium-dependent relaxation of mesenteric lymphatic vessels. *Microcirculation.* **21:** 640–648.
38. Breslin, J. W. 2011. ROCK and cAMP promote lymphatic endothelial cell barrier integrity and modulate histamine and thrombin-induced barrier dysfunction. *Lymphat. Res. Biol.* **9:** 3–11.
39. Nordestgaard, B. G., M. J. Chapman, S. E. Humphries, H. N. Ginsberg, L. Masana, O. S. Descamps, O. Wiklund, R. A. Hegele, F. J. Raal, J. C. Defesche, et al. 2013. Familial hypercholesterolaemia is underdiagnosed and undertreated in the general population: guidance for clinicians to prevent coronary heart disease: consensus statement of the European Atherosclerosis Society. *Eur. Heart J.* **34:** 3478–3490.
40. Schaefer, E. J., R. D. Santos, and B. F. Asztalos. 2010. Marked HDL deficiency and premature coronary heart disease. *Curr. Opin. Lipidol.* **21:** 289–297.
41. Ishibashi, S., J. L. Goldstein, M. S. Brown, J. Herz, and D. K. Burns. 1994. Massive xanthomatosis and atherosclerosis in cholesterol-fed low density lipoprotein receptor-negative mice. *J. Clin. Invest.* **93:** 1885–1893.
42. Joyce, C. W., E. M. Wagner, F. Basso, M. J. Amar, L. A. Freeman, R. D. Shamburek, C. L. Knapper, J. Syed, J. Wu, B. L. Vaisman, et al. 2006. ABCA1 overexpression in the liver of LDLr-KO mice leads to accumulation of pro-atherogenic lipoproteins and enhanced atherosclerosis. *J. Biol. Chem.* **281:** 33053–33065.
43. Wang, N., D. Lan, W. Chen, F. Matsuura, and A. R. Tall. 2004. ATP-binding cassette transporters G1 and G4 mediate cellular cholesterol efflux to high-density lipoproteins. *Proc. Natl. Acad. Sci. USA.* **101:** 9774–9779.
44. Escolà-Gil, J. C., G. Llaverias, J. Julve, M. Jauhiainen, J. Mendez-Gonzalez, and F. Blanco-Vaca. 2011. The cholesterol content of Western diets plays a major role in the paradoxical increase in high-density lipoprotein cholesterol and upregulates the macrophage reverse cholesterol transport pathway. *Arterioscler. Thromb. Vasc. Biol.* **31:** 2493–2499.
45. Pejler, G., E. Ronnberg, I. Waern, and S. Wernersson. 2010. Mast cell proteases: multifaceted regulators of inflammatory disease. *Blood.* **115:** 4981–4990.
46. Bot, I., G. P. Shi, and P. T. Kovanen. 2014. Mast Cells as Effectors in Atherosclerosis. *Arterioscler. Thromb. Vasc. Biol.* Epub ahead of print. August 7, 2014; doi:10.1161/ATVBAHA.114.303570.
47. Judström, I., H. Jukkola, J. Metso, M. Jauhiainen, P. T. Kovanen, and M. Lee-Rueckert. 2010. Mast cell-dependent proteolytic modification of HDL particles during anaphylactic shock in the mouse reduces their ability to induce cholesterol efflux from macrophage foam cells ex vivo. *Atherosclerosis.* **208:** 148–154.
48. Kokkonen, J. O., and P. T. Kovanen. 1987. Stimulation of mast cells leads to cholesterol accumulation in macrophages in vitro by a mast cell granule-mediated uptake of low density lipoprotein. *Proc. Natl. Acad. Sci. USA.* **84:** 2287–2291.
49. Kaartinen, M., A. Penttilä, and P. T. Kovanen. 1995. Extracellular mast cell granules carry apolipoprotein B-100- containing lipoproteins into phagocytes in human arterial intima. Functional coupling of exocytosis and phagocytosis in neighboring cells. *Arterioscler. Thromb. Vasc. Biol.* **15:** 2047–2054.